Vietnam Journal of Mechanics, Vol. 45, No. 2 (2023), pp. 117 – 130
DOI: https://doi.org/10.15625/0866-7136/17662

NUMERICAL SIMULATION OF SPRINGBACK AND TWISTING OF STAMPED THIN U-SHAPED COPPER ALLOY SHEETS WITH A CHANGE OF THE BLANK ALIGNMENT

Giap Xuan Ha[1,*]
[1]*Department of Engineering and Technology, Hong Duc University, Thanh Hoa, Vietnam*
[*]E-mail: haxuangiap@hdu.edu.vn

Received: 16 November 2022 / Published online: 30 June 2023

Abstract. An experimental database of springback and twisting of U-shaped elongated structures is available from a previous study. The materials are copper alloys: pure Cu, CuBe2, and CuFe2P, provided in thin sheets of thickness around 0.1 mm. After deep-drawing of rectangular blanks, which can be aligned with the tools or slightly misaligned, and tool withdrawal, the U-shaped structure exhibits an opening of the section (2D springback) and twisting (3D springback). Characteristic features of the deformed geometry are significantly different for the three alloys. This study is directed to understand the origin of that difference with a numerical simulation of the process. The mechanical behaviour of the materials was investigated in tension and hydraulic bulge test, out of comparison's sake and to derive the hardening law over a strain range representative of the process. Finite element simulations are performed using the von Mises criterion coupled with isotropic hardening, to compare the predicted forming load and springback parameters with experimental values.

Keywords: copper alloys, thin sheet metal, deep drawing, springback, twisting.

1. INTRODUCTION

Copper alloys are commonly employed in the electronic industry for their remarkable electrical and mechanical properties, e.g. leadframes (or substrates) supporting the chip and the leads that electrically connect the part to its environment [1]. They are used as sheet materials with thicknesses ranging from about 1 mm down to about 0.1 mm, depending on the application and current intensity. Such parts are usually obtained via a succession of cutting and forming steps, the latter being dominated by bending over small radii [2]. One of the main issues is therefore to control and/or compensate springback. Indeed, the prediction of the final shape is essential to ensure the quality and

durability of the connections with the components welded or clipped on the substrate. It is now well established that virtual forming can decrease the design step, as long as the mechanical behaviour used as the input in the numerical models is reliable [3]. Though springback prediction is still a matter of scientific investigation, it has been shown that the influence of the constitutive model is high, as well as the process parameters, in order to control the input parameters of the numerical model. Springback prediction has been widely investigated for parts in the automotive industry, with a focus on steels and aluminium alloys, but much less for copper alloys [4–7]. The aim of this paper is therefore to bring about 2D and 3D springback predictions after drawing of a U-shaped channel for 3 different copper alloys.

Springback can be classically split into 2D springback, corresponding to a change in the section geometry, i.e. angular change and sidewall curl for channel-type parts, and 3D springback or twisting (also called torsional springback). Twisting is qualified by a torsion of the elongated part around an axis parallel to its highest dimension [8]. Although there have been considerable studies oriented towards the angle change and curl springback characteristics, there is a shortage of research on the twisting of sheet metals as yet. The twisting of various thin curved rails made of 4 advanced high-strength steel materials is investigated with consideration of the tool design and process parameters such as cross-section width ratio, corner angle, draw-bead depth, and steel grades [9]. It was found that torsion was the most influent factor. Twisting, investigated on curved U channels, is dependent on the shear stress in the flange and sidewall regions arising in the drawing process and the opening as well as the curl of the sidewall due to the springback [10]. On account of in-plane deformation of the flanges and walls during the process, shear stress got higher when the drawing ratios were larger. Twisting also arises from the misalignment of rectangular blanks with the forming tools, whereas only 2D springback occurs for aligned blanks [11]. The numerical prediction of twisting is also a matter of interest and is classically influenced by the input data for the material mechanical behaviour [12] and elastic deformation of the tools [13].

An experimental database related to the 2D and 3D springback of channels made of copper alloy sheets, with a thickness around 0.1 mm, is detailed in [14] for 3 sheet materials, i.e. pure copper (99.9%), copper-beryllium (CuBe2) and copper-iron (CuFe2P) alloys. Of these, the electrical resistivity increases with alloying, also do the mechanical properties. The deformed shape after springback is measured with a 3D laser scanner, which exposes considerable dissimilarities in springback parameters between the blanks having identical dimensions but different materials, yet the modelling and simulation for them are still lacking. This study aims to investigate numerically the influence of the material on the springback magnitude. Moreover, specific tests to characterise 2D

springback, with the same rig but aligned blanks with the tools, are also presented and added to the experimental database, to compare with the numerical predictions.

2. FORMING EXPERIMENTS

To study the springback behaviors and parameters of U-shaped copper alloy sheets, Thuillier et al. [14]. and Pham et al. [12, 15] accomplished deep-drawing tests on many elongate samples, which are reiterated as below.

To form U-shaped specimens for each material, four copper alloy blank samples were prepared with a rectangular shape of dimensions 100 mm $\times$ 28 mm, with the largest dimension parallel to the rolling direction. In fact, the anisotropy of the materials was found to have only a neglected effect on the final geometry of the specimens, therefore in a first step, it is not taken into account. The scheme of the deep drawing is shown in Fig. 1. Every blank is be drawn to a depth of 7 mm, and it is intentionally misaligned by 2° with respect to the tools to enhance the twisting phenomenon. This misalignment helps form an asymmetric part with respect to the direction parallel to the part length, as such that each end section of the blank has a short flange and a long one, while the middle section is still symmetrical [14]. As the blank is not symmetric, two identical shims are inserted between it and the die to smooth the holding force and enhance the stability. Each shim has dimensions of 100 mm $\times$ 24 mm, while its material and thickness are the same as those of the blank. The blank holder force is applied on the blank and on two shims; it is kept constant throughout the drawing process, at the same value of 23 kN for each material. Initially, the section of the blank and shims lying beneath the blank holder is such that the corresponding pressure on the blank is around 3.5 MPa [12].

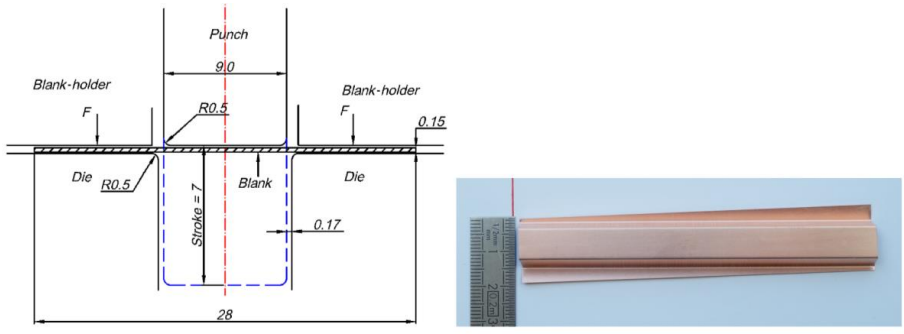

Fig. 1. Drawing scheme (left) and a sample after springback (right) in the misaligned case [14]

The final geometry of the drawn parts is measured using a laser scanner fixed on a 3D measuring machine; a data-point cloud, from the extraction of the node coordinates on three sections selected along the specimen's length, is generated and post-treated. 2D

springback of each section is analysed. Essentially, it is determined by three factors: (i) the angle θ_1 between the bottom and the wall, (ii) the angle θ_2 between the wall and the flange, and (iii) the curvature radius ρ of the wall of the section (see Fig. 2) [15].

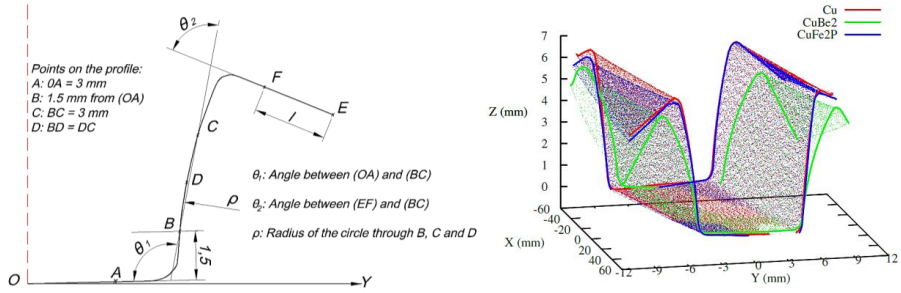

Fig. 2. Springback parameters description (left) and comparison of the deformed shape for the three materials (right) [11]

Moreover, specimens with smaller dimensions, i.e. 36 mm $\times$ 45 mm, are also considered but the blanks are formed with no misalignment of the tools, to investigate only 2D springback or section opening. In this alignment case, the corresponding pressure on the blank holder is around 2 MPa. Images of the deformed parts are shown in Fig. 3. In this case, the blank is laid symmetrically, ensuring a balance of the holding force, so no shims are necessary.

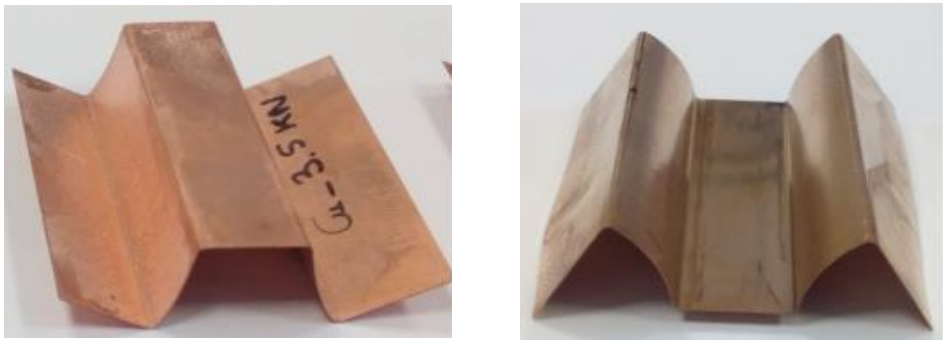

(a) Pure copper (b) CuBe2

Fig. 3. Images of deformed part shape after drawing and springback of 2 copper alloys: aligned case. Scale: the length of the part is 36 mm

3. FINITE ELEMENT SIMULATIONS

The aim of this section is to present the finite element models, for both aligned and misaligned cases. Thereby, the phenomenological theory of plasticity is employed. In the

first step, and out of comparison's sake between the three materials, a simple mechanical model, i.e isotropic hardening associated with the von Mises yield criterion, is considered. Then 3D and 2D numerical models are detailed, corresponding to the misaligned and aligned cases.

3.1. Mechanical properties of the materials

Tensile tests were performed, as well as hydraulic bulge tests, to investigate the hardening behaviour over a large strain range. The detailed implementation can be found in [14, 16]. The mechanical properties are given in Table 1 and the hardening curve giving the evolution of the equivalent (Cauchy) stress as a function of the equivalent plastic strain is presented in Fig. 4.

Table 1. Mechanical properties measured in the tension of the 3 copper alloys [14]

Materials	Young's modulus E (GPa)	Yield strength $R_{p0.2\%}$ (MPa)	Ultimate tensile stress R_m (MPa)	Normal anisotropy coefficient $\bar{r}$	Planar anisotropy variation Δr
Cu 9.9%	104	186	253	0.69	0.08
CuFe2P	114	335	419	0.60	0.15
CuBe2	126	385	518	0.92	0.28

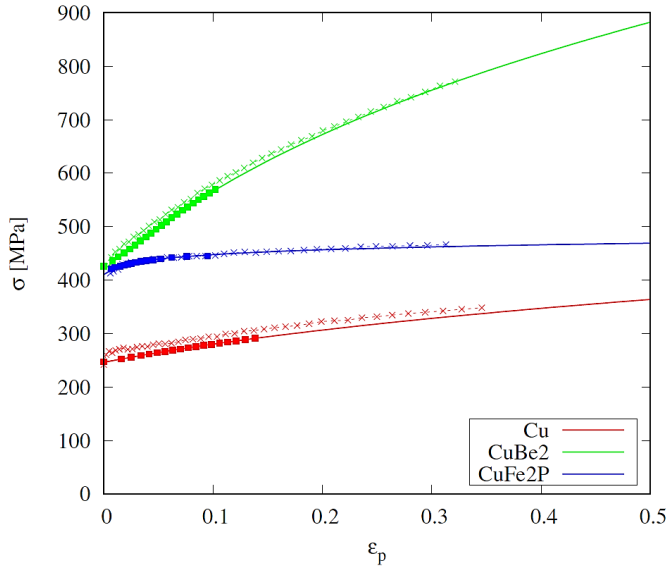

Fig. 4. Hardening curves (Cauchy stress σ - equivalent plastic strain ε_p) for the 3 copper alloy: Tensile tests (squares); bulge tests (crosses with dashes); extrapolated data (solid line) [2]

It can be seen that not only the initial stress is different for the materials, but also the subsequent hardening. Indeed, copper alloys are often subjected to thermo-mechanical treatments, after rolling, to reach the prescribed mechanical properties. CuFe2P alloy exhibits a rather low strain hardening, whereas it is higher for pure Cu and much higher for CuBe2 [14].

3.2. Numerical modelling

Misaligned case. Since the blank is intentionally misaligned by 2° with respect to the tools to enhance the twisting phenomenon, the deep drawing process has no axis of symmetry. Thus, the forming process of the blank is simulated with a 3D model with Abaqus finite element software. In practice, 2 shims having the same material as the blank are inserted to ensure a homogeneous distribution of the blank holder pressure, so they actually behave like deformable bodies and are included in the modelling. All components and their position in the numerical model are shown in Fig. 5; the tools are defined as analytical rigid bodies, and the blank as well as the shims are 3D deformable parts. The explicit framework is chosen for the deep drawing simulation, while the implicit framework is used for the subsequent springback step. Two points of the blank need to be constrained during the removal of the tools: one node in the middle of the bottom surface is pinned and the node opposite to it across the blank thickness is fixed along 2 directions (X and Y) [17].

In every case of contact interaction, surface-to-surface model is used. This kind of contact helps to specify different friction coefficients between surface pair. Overall, all contacts between the tools and the blank as well as the shims should have tangential behaviour that permits some relative motion of the surfaces. The kinematic contact method is imposed for the contact between the blank and the punch since it is able to keep the contact more stable, while the penalty contact method is used for other contacts between the blank and the holders and the die.

Similar to the experiment, the applied blank holder force is set equal to 23 kN and kept constant from the beginning up to a punch stroke of 7 mm. The drawing process is simulated in quasi-static conditions to avoid oscillations, so a smooth amplitude is applied to the punch displacement. The frictions between the blank and the planar surfaces and fillet surfaces of the tools are different to each other, which are calibrated from the punch load evolution in the experiment. For the deep drawing simulation of the blanks, the former friction is set at 0.50 and the latter friction is set at 0.65, respectively.

To mesh the blank, 8-node linear brick element with reduced integration (C3D8R) is used. This element type takes account of shear stress through the thickness, so it is much better than continuum shell element in predicting springback and twisting. However,

C3D8R element exhibits several considerable shortcomings that need to be manipulated as follows:

(i) The element tends to be not stiff enough in bending, so the mesh must be finer at such positions.

(ii) Stresses and strains are most accurate at the integration points. Because C3D8R element's integration point lies in the middle of the element, it is obligatory to utilize small elements to catch a stress concentration at the edge of a structure.

(iii) There are 12 spurious zero energy modes leading to a massive hourglass. For these reasons, the blank is meshed with four layers of elements through the thickness, and the option 'relax stiffness hourglass control' is considered, as it tends to bring about more accurate solutions when high distortion occurs [18].

After being meshed, the blank is rotated around the vertical axis 2° to obtain the initial misalignment, so that the blank mesh is also misaligned with respect to the tool extrusion direction (X direction in the 3D model). Not only does this misalignment help to facilitate twisting of the blank at the end, but also it prevents oscillations on the load prediction, which are related to the simultaneous gliding of rows of nodes over the die radius as shown for the aligned case. To optimise the computation time, the mesh seed sizes of the blank are biased. Namely, the blank is divided into five partitions by its width: two flanges, two walls, and the bottom. The mesh seeds of the flanges and walls bias from 0.07 mm to 0.12 mm, while the mesh seeds of the bottom bias from 0.07 mm to 0.25 mm. Along the length (100 mm) of the blank, the mesh seed is uniform and equal to 0.04 mm.

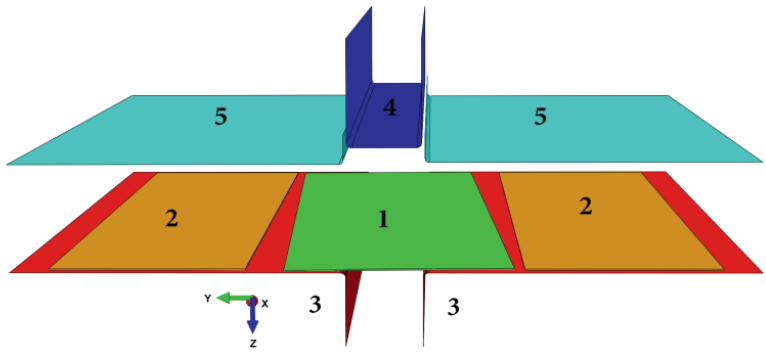

Fig. 5. Plan of the blank (1), shims (2), die (3), punch (4) and blank holder (5) in the numerical model for the misaligned case [12]

The C3D8R elements were also used to mesh the shims. Because both shims always deform uniformly, one layer through the thickness of elements with dimensions of 2 mm $\times$ 2 mm is assigned.

Aligned case. For the misaligned case, numerical simulations are performed using Abaqus, but only the implicit scheme is used for the drawing and springback. The tools are rigid bodies and from the symmetry conditions, only a 2D model is considered in plane strain considering the length of 36 mm. Therefore, plane strain bilinear finite element with 4 nodes and reduced integration is used to mesh the part, with 3 layers in the thickness. The friction coefficient between the tools and the blank is constant and equal to 0.50. Linear extrapolation of the hardening above the maximum homogeneous strain in tension is considered, associated with Hill's 1948 yield criterion, which parameters are identified from the data in Table 1.

4. RESULTS

The comparison between experiments and numerical simulation is performed on the load and 2D and, when relevant, 3D springback parameters.

4.1. Load predictions

Fig. 6 shows a comparison of the load levels normalised by the initial thickness, as the material CuFe2P has a slightly higher thickness than the other two materials. The result highlights the strong influence of the copper alloy materials: the higher the flow stress in tension, the higher is the forming load. However, CuFe2P exhibits the highest

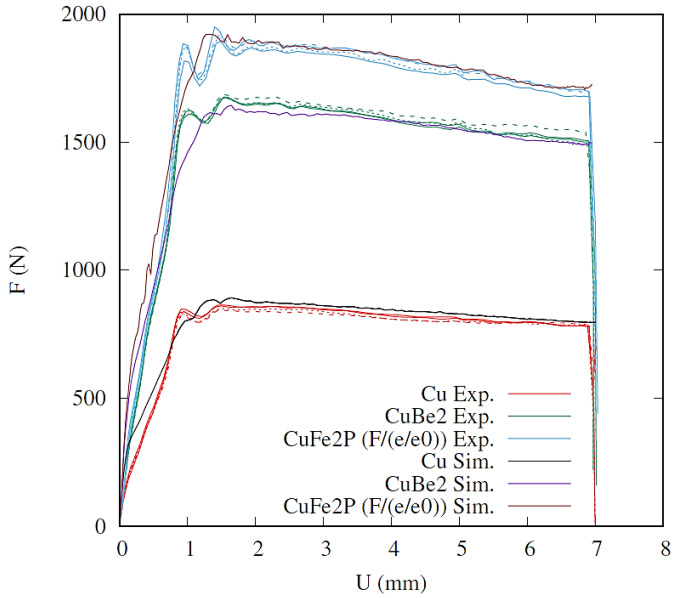

Fig. 6. Comparison of the forming loads F as a function of the punch stroke U for the three materials in the misaligned case (four samples and one simulation model for each material)

load though CuBe2 has the highest hardening rate and reaches the highest stress level in tension for an equivalent plastic strain around 0.16 (see Fig. 4 again), which corresponds to the maximum strain obtained at the end of the drawing process. This phenomenon may come from the friction and indeed, values of the friction coefficients for CuFe2P in the numerical model had to be increased compared to the other two materials. It can be seen that the 3D model reproduces well the load evolution, exhibiting a steady decrease after the initial peak value, whereas in 2D, the load remains rather constant. For all simulations, the friction coefficient is adjusted at the load level. It was found, for the same test but stainless steel [5], that different values of the friction coefficient for the planar surfaces and for the radii of the punch and die lead to a better description of the whole evolution of the load with the punch stroke.

4.2. 2D springback parameters

The geometry of three sections, i.e. the middle one and the 2 extreme ones for the 3D case, and only the middle one in the 2D case, is analysed by calculating angles θ_1, θ_2, and the curvature radius of the wall ρ. Fig. 7 shows a comparison between experimental and numerical values for the three materials and the misaligned case; the same scale is used for the three materials to facilitate the comparison. The values are presented for the 4 tests, to highlight the repeatability, and on the right-hand-side of each graph, for the numerical simulation. The 2 extreme sections have both a long and short flange, due to the dissymmetry but not on the same side, whereas the middle section is symmetric.

Overall, pure copper and CuFe2P exhibit similar trends, i.e. θ_1 and θ_2 are respectively of the order of 100–105° and 85°, with a fairly good prediction for pure copper of θ_1 but a slight overestimation for θ_2. The parameters for CuFe2P are either slightly overestimated for θ_1 or underestimated for θ_2. For CuBe2, the average experimental values for θ_1 and θ_2 are respectively 120° and 76°. The evolution of θ_1 as a function of the flange length is not well predicted, with a roughly constant value. A similar underestimation is noted for θ_2.

Concerning the wall curvature radius ρ, the order of magnitude is well predicted for the three materials, though the huge increase recorded for pure copper and CuFe2P for the short flange (70 mm for pure copper and up to 80 mm for CuFe2P) is not predicted. However, the rather straight walls obtained for this material lead to high ρ values, that are very sensitive to the process parameters and lead to a rather large dispersion. Section opening for CuBe2 is large compared to that for the other two materials, being indicated by a slight value of the wall curvature. Namely, ρ is about 8 mm and independent of the flange dimension, which is well predicted in the simulation.

As a whole, the numerical predictions reflect correctly that pure copper and CuFe2P have 2D springback magnitude lower than that of CuBe2.

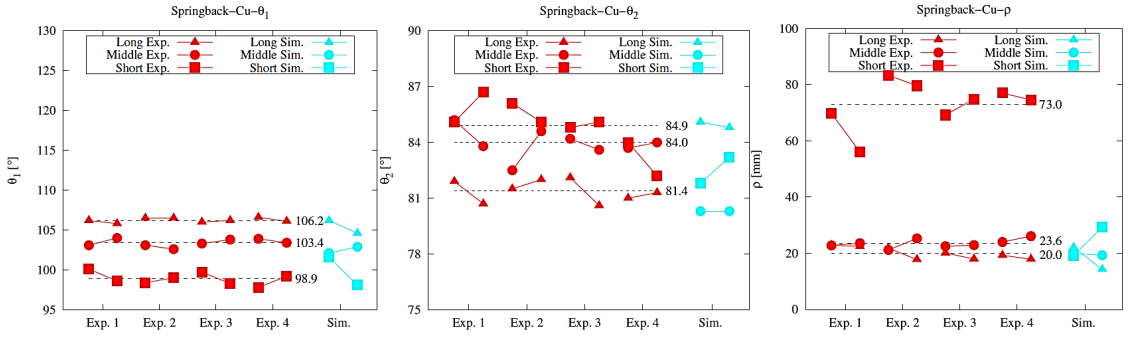

(a) Pure copper

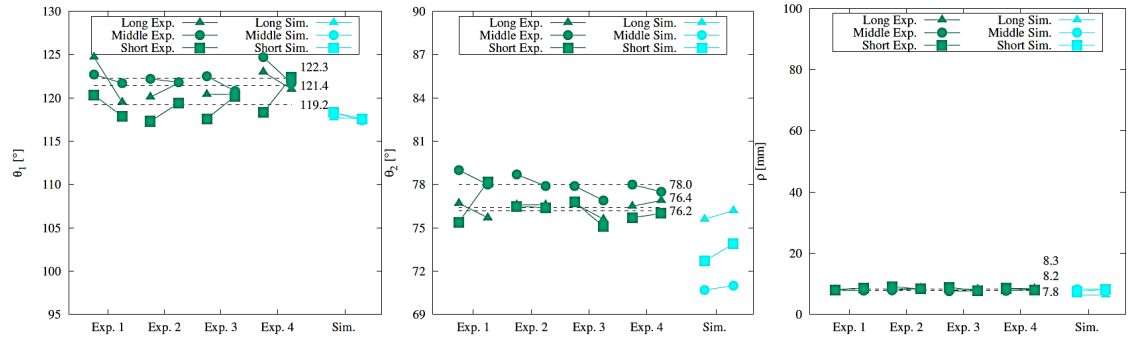

(b) CuBe2

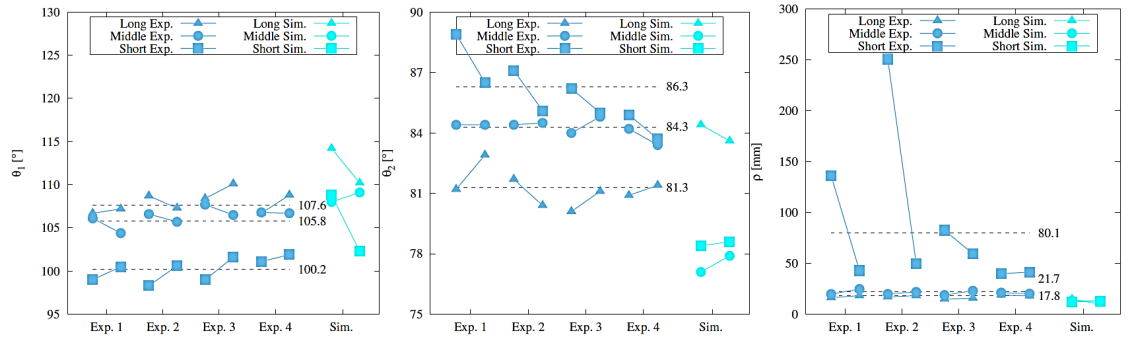

(c) CuFe2P

Fig. 7. Prediction of the geometric parameters describing the section shape after springback, for the misaligned case (Dash line: the average)

Fig. 8 presents the comparison of the experimental and predicted values for the parameters θ_1 and θ_2, for the aligned case. It can be seen that the order of magnitude of the first one is rather close to the value obtained for the misaligned case, i.e. 105° and 115–120° respectively for pure copper and CuBe2; whereas θ_2 values are significantly lower,

70° and 50° respectively for pure copper and CuBe2, to be compared with respectively 85° and 75° for the misaligned case. This difference could come from the blank geometry (longer flange length for the aligned case compared to the misaligned one) or also from the twisting phenomenon occurring in the misaligned case. Finally, the influence of the blank holder force on the springback is rather well predicted, as well as the order of magnitude of the two parameters.

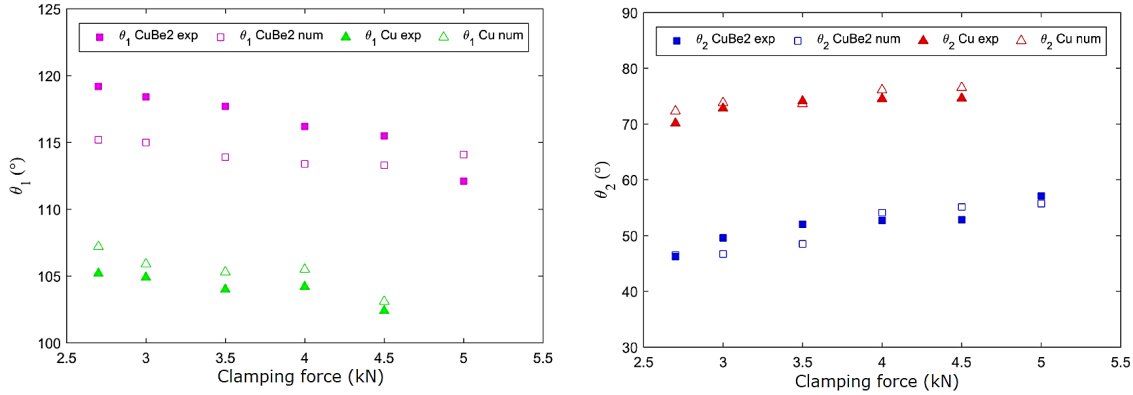

(a) Parameter θ_1 (b) Parameter θ_2

Fig. 8. Prediction of the geometric parameters describing the section shape after springback, for the aligned case

The predictions are expected to be improved when using a more advanced modelling for the mechanical behaviour, i.e. taking account the Baushinger effect exhibited by these materials.

4.3. Twisting

Though pure copper and CuFe2P exhibit rather low 2D springback magnitude, 3D springback magnitude is higher for these two materials than for CuBe2. Such magnitude is characterised by a twisting parameter, defined as the ratio of the angle between the bottom line of the two end sections to the distance between them. Fig. 9 compares the predicted twisting parameter with experimental values, for the misaligned case, obtained from the same four tests provided in Section 2. The good repeatability, analysed over 4 tests for each material, must be highlighted, leading to reliable average values of respectively $28°m^{-1}$, $8°m^{-1}$ and $45°m^{-1}$ for pure copper, CuBe2 and CuFe2P. For pure copper and CuFe2P, it can be seen that the higher 3D springback is, the lower 2D springback (the section opening) is. The numerical prediction of the twisting parameter is appropriate for CuBe2 but overestimated for pure copper and CuFe2P.

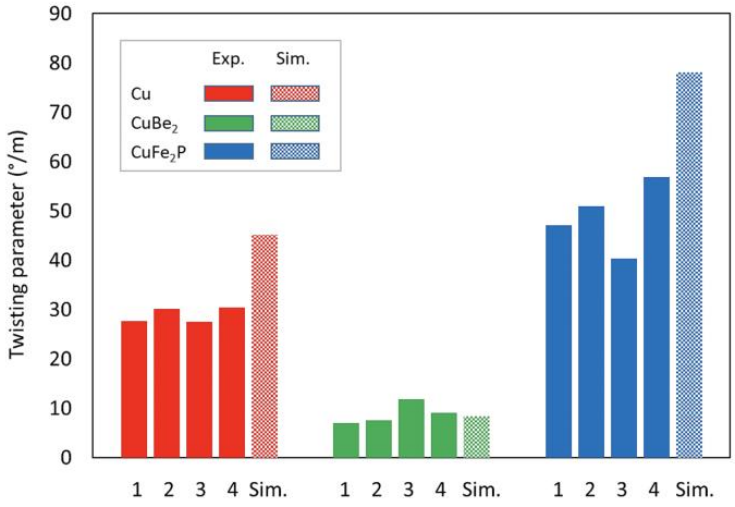

Fig. 9. Twisting parameters for the three materials. For each material, the first 4 values stand for the experiments and the last one for the numerical simulation

However, the trend that low 2D springback magnitude is associated with a high twist is well captured. This trend may be related to the hardening rate of the material. Indeed, as shown in Fig. 4, CuBe2 exhibits a large hardening rate, compared to the other two materials. That is exhibited as CuBe2 samples have the biggest average of θ_1 and the smallest averages of θ_2, ρ, and the twisting parameter. This correlation demands a further investigation.

5. CONCLUSION

This study presents a comparison of experimental and numerical results related to 2D and 3D springback of 3 copper alloys. A drawing process of U-shaped channels is considered, with rectangular blanks either aligned or slightly misaligned with the forming tools. The forming load and final shape after springback are analysed. In the first step, the mechanical behaviour of the materials is simply represented with isotropic hardening associated to von Mises yield criterion. It is shown that the numerical model accurately predicts the low 2D springback magnitude observed for pure copper and CuFe2P and the large section opening of CuBe2 and the rather large twist of the first two materials compared to the last one. This trend could be related to the hardening rate of the materials. However, the application of only phenomenological theory of plasticity has its drawback. Although the simulation renders proper prediction of punch load against the stroke, it does not provide a clear and deep insight of springback and twisting processes. It is expected to improve the numerical predictions with a more advanced model in the theory of dislocation-mediated plasticity as employed in [19–21].

ACKNOWLEDGMENTS

The author is grateful to the IRDL of the University Bretagne Sud for profound advice on fabricating and examining copper-based samples.

DECLARATION OF COMPETING INTEREST

The authors declare that they have no known competing financial interests or personal relationships that could have appeared to influence the work reported in this paper.

FUNDING

This research received no specific grant from any funding agency in the public, commercial, or not-for-profit sectors.

REFERENCES

[1] Copper and Copper Alloys. *General information - introduction to copper and its alloys*. Accessed Nov. 09, 2022.

[2] G. X. Ha, M. G. Oliveira, A. Andrade-Campos, P. Y. Manach, and S. Thuillier. Prediction of coupled 2D and 3D effects in springback of copper alloys after deep drawing. *International Journal of Material Forming*, **14**, (2021), pp. 1171–1187. https://doi.org/10.1007/s12289-021-01631-x.

[3] H. B. Mullan. Improved prediction of springback on final formed components. *Journal of Materials Processing Technology*, **153-154**, (2004), pp. 464–471. https://doi.org/10.1016/j.jmatprotec.2004.04.384.

[4] C. Gomes, O. Onipede, and M. Lovell. Investigation of springback in high strength anisotropic steels. *Journal of Materials Processing Technology*, **159**, (2005), pp. 91–98. https://doi.org/10.1016/j.jmatprotec.2004.04.423.

[5] V. Esat, H. Darendeliler, and M. I. Gokler. Finite element analysis of springback in bending of aluminium sheets. *Materials & Design*, **23**, (2002), pp. 223–229. https://doi.org/10.1016/s0261-3069(01)00062-0.

[6] P. Chen and M. Koç. Simulation of springback variation in forming of advanced high strength steels. *Journal of Materials Processing Technology*, **190**, (2007), pp. 189–198. https://doi.org/10.1016/j.jmatprotec.2007.02.046.

[7] H.-L. Dai, H.-J. Jiang, T. Dai, W.-L. Xu, and A.-H. Luo. Investigation on the influence of damage to springback of U-shape HSLA steel plates. *Journal of Alloys and Compounds*, **708**, (2017), pp. 575–586. https://doi.org/10.1016/j.jallcom.2017.02.270.

[8] M. Dezelak, A. Stepisnik, and I. Pahole. Evaluation of twist springback prediction after an AHSS forming process. *International Journal of Simulation Modelling*, **13**, (2014), pp. 171–182. https://doi.org/10.2507/ijsimm13(2)4.261.

[9] H. Li, G. Sun, G. Li, Z. Gong, D. Liu, and Q. Li. On twist springback in advanced high-strength steels. *Materials & Design*, **32**, (2011), pp. 3272–3279. https://doi.org/10.1016/j.matdes.2011.02.035.

[10] M. Takamura, M. Sakata, A. Fukui, T. Hama, Y. Miyoshi, H. Sunaga, A. Makinouchi, and M. Asakawa. Investigation of twist in curved hat channel products by elastic-plastic finite element analysis. *International Journal of Material Forming*, **3**, (2010), pp. 131–134. https://doi.org/10.1007/s12289-010-0724-1.

[11] C. H. Pham, S. Thuillier, and P. Y. Manach. Twisting analysis of ultra-thin metallic sheets. *Journal of Materials Processing Technology*, **214**, (2014), pp. 844–855. https://doi.org/10.1016/j.jmatprotec.2013.12.006.

[12] C. H. Pham, S. Thuillier, and P.-Y. Manach. 2D springback and twisting of ultra-thin stainless steel U-shaped parts. *steel research international*, **86**, (2015), pp. 861–868. https://doi.org/10.1002/srin.201400569.

[13] A. Ishiwatari, H. Kano, J. Hiramoto, and T. Inazumi. Improvement on CAE model for accurate torsional springback prediction in high strength steel part forming. *Key Engineering Materials*, **504-506**, (2012), pp. 437–442. https://doi.org/10.4028/www.scientific.net/kem.504-506.437.

[14] S. Thuillier, C. H. Pham, and P. Y. Manach. 2D springback and twisting after drawing of copper alloy sheets. *Journal of Physics: Conference Series*, **1063**, (2018). https://doi.org/10.1088/1742-6596/1063/1/012124.

[15] C. H. Pham, S. Thuillier, and P. Y. Manach. Twisting of sheet metals. In *AIP Conference Proceedings*, AIP, Vol. 1567, (2013), pp. 422–427. https://doi.org/10.1063/1.4850005, https://doi.org/10.1063/1.4850005.

[16] F. Adzima, T. Balan, P. Y. Manach, N. Bonnet, and L. Tabourot. Crystal plasticity and phenomenological approaches for the simulation of deformation behavior in thin copper alloy sheets. *International Journal of Plasticity*, **94**, (2017), pp. 171–191. https://doi.org/10.1016/j.ijplas.2016.06.003.

[17] S. T. C. H. Pham and P.-Y. Manach. Experimental investigation and numerical prediction of twisting. In *Proceedings of IDDRG 2014 Conference*, Paris, France, (2014).

[18] C3D8R and F3D8R. *http://web.mit.edu/calculix_v2.7/CalculiX/ccx_2.7/doc/ccx/node27.html*. Accessed Oct. 09, 2022.

[19] J. S. Langer, E. Bouchbinder, and T. Lookman. Thermodynamic theory of dislocation-mediated plasticity. *Acta Materialia*, **58**, (2010), pp. 3718–3732. https://doi.org/10.1016/j.actamat.2010.03.009.

[20] K. C. Le, Y. Piao, and T. M. Tran. Thermodynamic dislocation theory: Torsion of bars. *Physical Review E*, **98**, (2018). https://doi.org/10.1103/physreve.98.063006.

[21] K. C. Le and T. M. Tran. Thermodynamic dislocation theory: Bauschinger effect. *Physical Review E*, **97**, (2018). https://doi.org/10.1103/physreve.97.043002.